Enhanced Vaccine Design Strategies for Toxoplasmosis: A Computational Analysis of Toxoplasma gondii Rhoptry Protein 13 (ROP13)

Running head: Rhoptry Protein 13 (ROP13) as *Toxoplasma gondii* vaccine target

Leila Zaki[1], Aida Vafae Eslahi[1], Masoud Foroutan[2,3], Majid Pirestani[4], Kareem Hatam-Nahavandi[5], Amir Karimipour-saryazdi[4], Mohammad Ghaffari Cherati[1], Daniel Diaz[6], Milad Badri[1,*]

[1]Medical Microbiology Research Center, Qazvin University of Medical Sciences, Qazvin, Iran

[2]Research Center for Environmental Contaminants (RCEC), Abadan University of Medical Sciences, Abadan, Iran

[3]Department of Basic Medical Sciences, Faculty of Medicine, Abadan University of Medical Sciences, Abadan, Iran

[4]Department of Parasitology and Entomology, Faculty of Medical Sciences, Tarbiat Modares University, Tehran, Iran

[5]Department of Parasitology and Mycology, School of Medicine, Iranshahr University of Medical Sciences, Iranshahr, Iran

[6]Facultad de Ciencias, Universidad Nacional Autónoma de México, Av. Universidad 3000, Copilco, Coyoacán 04510, Ciudad de México, México

Leila Zaki, Aida Vafae Eslahi and Masoud Foroutan contributed equally to this work.

[*]Corresponding author:

Milad Badri (badri22.milad@gmail.com)

preprint

Abstract

Toxoplasma gondii (T. gondii), an intracellular parasite, utilizes a variety of rhoptry proteins (ROPs) to facilitate invasion and interactions with host cells. Among these ROPs, Rhoptry Protein 13 (ROP13) stands out for its expression in both bradyzoite and tachyzoite forms of *T. gondii* and its ability to engage with various host cytoplasmic compartments. In this bioinformatics study, we employed a range of tools to predict the fundamental characteristics of the ROP13 protein.Our analysis revealed that the ROP13 protein consists of 400 amino acid residues with an average molecular weight (MW) of 44,714.15 Daltons. The grand average of hydropathicity (GRAVY) was determined to be -0.311, indicating the protein's hydrophilic nature, while the aliphatic index scored 84.40, highlighting its hydrophobic properties. Furthermore, we identified 43 post-translationally modified sites within the ROP13 sequence. When examining the secondary structure, the ROP13 protein was predicted to have a composition of 40% alpha-helix, 9.25% extended strand, and 50.75% random coil using the GOR4 method, suggesting a diverse structural organization that may contribute to its functional versatility. Additionally, our analysis identified several potential B- and T-cell epitopes within the ROP13 sequence, indicating regions that could be targeted for immune responses.

Overall, the bioinformatics analysis of ROP13 provides valuable insights into its structural, immunogenic, and antigenic properties, highlighting its potential as a target for vaccine development against toxoplasmosis. By leveraging the predicted characteristics of ROP13, researchers can explore various vaccine strategies to enhance host immunity and combat *T. gondii* infection effectively. Continued investigation into the molecular mechanisms underlying ROP13's interactions with host cells will further elucidate its role in toxoplasmosis pathogenesis and guide the development of innovative approaches to mitigate this prevalent parasitic disease.

Keywords: *Toxoplasma gondii*, Rhoptry protein 13, *In silico*

1.1. Introduction

Toxoplasma gondii is a widely distributed protozoan parasite posing a significant public health concern, with an estimated one-third of the global population exposed to this parasite (1,2).

The life stages of *T. gondii* consist of a sexual phase and an asexual phase, which exclusively occur in the feline species (definitive hosts) and any warm-blooded animal (intermediate hosts), respectively (3–5). Oocysts, shed through the feces of definitive hosts, serve as the infectious stage

preprint

of *T. gondii*. Environmental, soil, and water contamination are the primary sources of infection (6). Accordingly, humans acquire the infection via contaminated drinking water or food, consumption of raw/undercooked meats containing latent cysts, vertical transmission, organ transplantation, and blood transfusion (6,7).

The clinical characteristics of toxoplasmosis are influenced by various factors, including the genotype of the protozoan and host-related characteristics such as age, gender, occupation, genetics, diet, immunological status, cultural behaviors, and contact with infected cats (8–10).

In immunocompetent individuals, *T. gondii* generally causes mild clinical manifestations, such as flulike symptoms, while in some humans with weak immune status (patients with HIV/AIDS, seronegative pregnant women, and organ transplant recipients), *T. gondii* infections cause serious disease, such as encephalitis, mental retardation, vision disorders, hydrocephalus, cerebral calcification, poor coordination, or may lead to death if not treated (11,12). *T. gondii* infection can lead frequent abortions, stillbirths, the birth of debilitated animals, and fetal death in some domestic animals, particularly sheep and goats. These outcomes result in significant economic disadvantages in animal husbandry settings and veterinary-related industries (13).

Toxoplasmosis is typically treated with chemotherapy that includes anti-malarial and antibacterial medications, which are the recommended drugs for managing the disease. Nevertheless, these agents have not been completely successful yet, and can have harmful side effects such as teratogenic traits, hypersensitivity, damaging some tissues, significant toxicity, potential parasite resistance as well as bone marrow suppression (14,15).

Since antiparasitic drugs have some limitations and are unable to eradicate bradyzoites in tissue cysts, discovering and design of secure and impressive vaccines are needed, particularly in humans and livestock animals. One of the significant challenges facing scientists in addressing *T. gondii* infection is the development of a useful and effective vaccine. To address this challenge, various immunization approaches with different formulations have been explored for toxoplasmosis. Recent vaccine development trials aimed at preventing *T. gondii* infection have primarily focused on antigens found on the parasite's major surface (SAGs), as well as proteins from micronemes (MICs), rhoptries (ROPs), and dense granules (GRAs) (16–19).

Among these different antigens, ROP protein family is a hoping vaccine candidate due to strong antigenicity and immunogenicity, as well as its ability to induce substantial immune responses (20,21). Several studies have assessed the efficacy of ROP antigens using different vaccine

preprint

platforms such as recombinant protein or DNA vaccines on the animal models in order to obtain favorable and promising results (18–21). As an excretory-secretory protein of *Toxoplasma gondii*, ROP13 has the ability to moderate immune response and therefore it shows great promise for application in immunization approaches against the infection (21). Furthermore, this protein exhibits strong immunogenicity similar to other ROPs and plays a crucial role in pathogenicity and survival within host cells (21–24).

Using *in silico* tools to predict vaccine targets is highly valuable as it enhances our understanding of these targets and allows for their rapid selection with careful consideration (25,26). Bioinformatics are the most successful prediction method for identifying effective epitopes and developing vaccine (25). These novel techniques are highly beneficial for analyzing proteins and assessing their structural, functional, immunogenic, biological, and biochemical characteristics as antigens (19,26). Therefore, the present study was designed aiming at identifying the essential biochemical characteristics and immunogenic epitopes of the ROP13 protein by utilizing various bioinformatics online servers.

2. Methods

2.1. Retrieval and initial assessment of the protein sequence

Initially, the amino acid sequence of ROP13 was obtained from the National Center for Biotechnology Information (NCBI) website (https://www.ncbi.nlm.nih.gov/protein/) in FASTA format.

2.2. Analysis of the physicochemical parameters of ROP13

The Expasy ProtParam (https: //web. expasy.org/protparam/) was utilized to assess the various physicochemical characteristics of ROP13, including amino acid composition, theoretical isoelectric point (pI), molecular weight (MW), total number of positively and negatively charged residues, extinction coefficients, instability index, aliphatic index, grand average of hydropathicity (GRAVY), and *in vitro* and *in vivo* half-life (27).

2.3. Projecting the post-translational modification (PTM) sites on ROP13

The online tools of NetPhos 3.1 (http://www.cbs.dtu.dk/services/NetPhos/) and CSS-Palm

preprint

((http://csspalm.biocuckoo.org/online.php) were used to determine the phosphorylation and acylation regions of the ROP13 protein, respectively (25).

2.4. The transmembrane domains and subcellular position of ROP13

The potential transmembrane regions (TMs) of ROP13 were evaluated using the TMHMM 2.0 (http://www.cbs.dtu.dk/services/TMHMM-2.0/). Additionally, the subcellular position of the protein was projected using the PSORT II (http://psort.hgc.jp/form2.html) (25).

2.5. The secondary and tertiary structure prediction

The secondary structure of ROP13 was anticipated using the Garnier-Osguthorpe-Robson (GOR) method through the online server (https://npsa-prabi.ibcp.fr/cgibin/npsa_automat.pl?page=npsa_gor4.html) (28). Afterward, the three-dimensional (3D) models of ROP13 sequence were generated using the SWISS-MODEL program, using a homology modeling approach (https://swissmodel.expasy.org/) (25,29).

2.6. Refinement and confirmation of the 3D modeled structure

The precision and quality of the generated models were determined through Ramachandran plot using SWISS-MODEL (https://saves.mbi.ucla.edu/) (30).

2.7. B-cell epitopes projection

To predict B-cell epitopes, the amino acid sequence of the ROP13 protein (accession no. AFH54221.1) was utilized. The ABCpred online server (http://crdd.osdd.net/raghava/abcpred/) was employed with a threshold of 0.75% to identify linear B-cell epitopes within the antigen sequence (31). To project the B-cell epitope, we utilized the Bcepred tool, which determines continuous B-cell epitopes based on physicochemical properties such as accessibility, polarity, hydrophilicity, turns, exposed surface, flexibility, and antigenic propensity was used (http://crdd.osdd.net/raghava/bcepred/bcepred_submission.html) (32).

Besides, the IEDB tool of the Immune Epitope Database (http://tools.iedb.org/bcell/) was employed to evaluate epitopes according to average flexibility, hydrophobicity, surface accessibility, antigenicity, alpha-helix and beta-turn. Eventually, conformational B-cell epitopes were appraised using ElliPro (http://tools.iedb.org/ellipro/) from the 3D epitope structure protein

preprint

data bank file by default parameters, comprising 0.5 min-score and 6 Å max distance. This server is able to predict the epitopes based on their protusion index (PI) values to estimate the protein shape, residual PI, and adjacent cluster residues (33).

2.8. MHC-I and MHC-II binding epitopes projection

The Immune Epitope Database (IEDB) was used to assess the half maximal inhibitory concentration (IC_{50}) of peptides derived from ROP13, which exhibit affinity to both major histocompatibility complex (MHC) class I and class II molecules. This was done using the recommended method provided by IEDB, accessible at the following links: for MHC class I molecules (http://tools.iedb.org/mhci/) and for MHC class II molecules (http://tools.immuneepitope.org/mhcii).

The MHC-I epitopes, each consisting of ten amino acids, were predicted using the mouse alleles H2-Ld, H2-Db, H2-Dd, H2-Kb, H2-Kd, and H2-Kk. For MHC-II epitope prediction, which involved 15 amino acids, the mouse alleles H2-IAb, H2-IAd, and H2-IEd were employed. The predictions were sorted by percentile rank (34,35).

2.9. Cytotoxic T lymphocyte (CTL) epitopes prediction

Identification of cytotoxic T-cell epitopes was accomplished using the CTLpred tool with performance accuracy of 75.8% (http://www.imtech.res.in/raghava/ctlpred/index.html). The prediction was done according to a consensus approach, previously described. The default parameters for the prediction were support vector machine of 0.36 and artificial neural network of 0.51 (36).

2.10. Evaluation of antigen probability, allergenicity, and solubility

The full ROP13 protein antigenicity was assessed initially with ANTI¬GENpro (http://scratch.proteomics.ics.uci.edu/) (37), and finally with VaxiJen v. 2.0 (http://www.ddg-pharmfac.net/vaxijen/) (38) web bases servers.

VaxiJen is used to predict conserved antigenic regions and it employs a novel alignment-free approach based on auto-cross covariance (ACC), which evaluates changes in peptide sequences to generate comparable vectors of primary amino acid features. The precision ranges between 70%

preprint

and 89%, based on the target organism (http://www. Ddg pharmfac.net/vaxijen/VaxiJen/VaxiJen_help.html).

Furthermore, the allergenic profile of ROP13 was projected using the AlgPred (http://www.imtech.res.in/raghava/algpred/) (39) with a hybrid methodology combining SVMc, IgE epitope prediction, ARPs BLAST, and MAST. AlgPred can project epitopes with 85% accuracy by comparing the identified epitope with protein regions, using a threshold of -0.4. The solubility of ROP13 was projected using the SOLpro server (http://scratch.proteomics.ics.uci.edu/) (40).

2.11. Immune simulation

The C-ImmSim was employed to predict the virtual immunological simulation process that was provoked by TgROP13 (https://150.146.2.1/C-IMMSIM/index.php?page=1). It was set for three inoculation doses of TgROP13 at four-week intervals with time points of 1, 84, and 168. Other settings for this computer-aided simulation included simulation volume 10, simulation steps 1050, and random seed 12345 (42).

3. Results

3.1. Gene and overall features of ROP13

The amino acid sequence of the ROP13 protein, acquired from NCBI in FASTA format (accession no. AFH54221.1).

According to ProtParam, the ROP13 protein consists of 400 amino acid residues with a predicted pI of 9.38 and a molecular weight of 44714.15 D. The ROP13 sequence contains 45 negatively charged residues (Asp + Glu) and 56 positively charged residues (Arg + Lys).

The extinction coefficient was measured to be 20440 M−1 cm−1 in water at 280 nm.

The estimated half-life of ROP13 was 30 hours in mammalian reticulocytes *in vitro*, over 20 hours in yeast *in vivo*, and over 10 hours in *Escherichia coli in vivo*.

preprint

Moreover, the instability index (II) of this protein indicates its unstable nature, with a score of 61.30. I addition, the GRAVY and aliphatic index were calculated to be -0.311 and 84.40, respectively.

3.2. PTM sites projection on ROP13

The results revealed that the ROP13 protein contains 41 phosphorylation sites (27 Ser, 14 Thr, and 0 Tyr) as shown in Figure 1A and B, along with 2 acylation sites listed in Table 1, indicating that there are a total of 43 PTM sites within our sequence.

```
    MKRTELCIAALVAVGAFAFTSPNAVAKSFERSLGHLDASSFLSSPLNSDV   #    50
    ELGRSTSPAQSPSFTEGTNETNPPTSRPPGRKYEGSDLHRRVAARHVEHK   #   100
    KRQEEWEQRKASRRSALTPSAPDPDGDGDPATSFPSQRRLLDRCLQQFRE   #   150
    QLVDWENLCKGSPEPDDCRSTVQEILANQSFGALHTTVISFSIFVNRDPR   #   200
    RLSFPVLDATDLRLTVKLKHLLDRIPGCAALSLPAYIGLVSSDVFKSEEF   #   250
    TRKVNRCSEDFGRSAREEPSRAGRAAAVVIRFMGLTPERQTFYQPFVFVT   #   300
    TQAAMLLSMVLKHPFLSILVNMACVAGGLCRKGIREVLLRALREADFQTE   #   350
    DVPLDSAPQELVDHLKMYLKLLFLRKYRRLRRQAANVAAQVVYANSLRLL   #   400
%1  ...T...............T.......S...S......SS..SS...S..   #    50
%1  .....TS...S.S.T.........TS........................   #   100
%1  ...........S..S..T.S...........TS..S..............   #   150
%1  ...........S........T........S....................   #   200
%1  ..S...........T.................S........SS....S...   #   250
%1  T......S.....S.....................T....T.........   #   300
%1  T...............S..............................T.   #   350
%1  ...............................................S....   #   400
```

A.

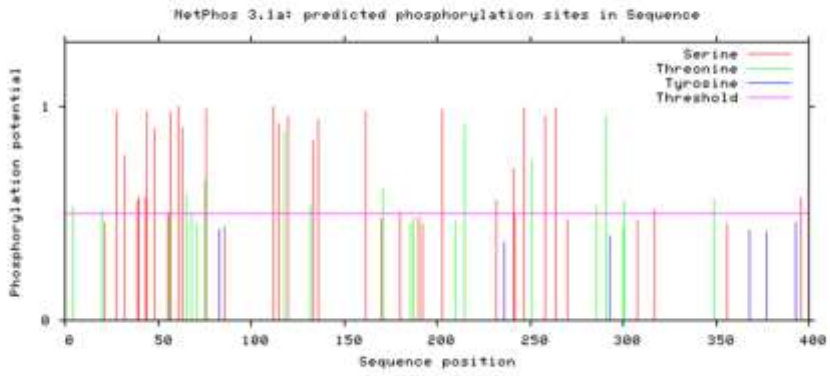

B.

Fig. 1. Bioinformatics analysis of the phosphorylation and acylation areas of the rhoptry protein 13(ROP13). (A) If the remnant is not phosphorylated, either because the score is below the threshold or because the residue is not S (serine), T (threonine), or Y (tyrosine), that posi- tion is marked by a dot ('.'). Residues having a prediction score

more than the threshold are indicated by 'S', 'T', or 'Y', respectively. (B) Expected phosphorylation positions in ROP13 sequence.

Table 1. The acylation sites of ROP13 sequence.

AFH54221.1	2	******MKRTELCIA	EP300	1.3	0.42
AFH54221.1	2	******MKRTELCIA	KAT2B	1.807	1.343
AFH54221.1	2	******MKRTELCIA	KAT8	8.9	7.222
AFH54221.1	82	TSRPPGRKYEGSDLH	KAT2A	1.638	1.382
AFH54221.1	82	TSRPPGRKYEGSDLH	KAT2B	1.798	1.343
AFH54221.1	100	AARHVEHKKRQEEWE	KAT8	7.5	7.222
AFH54221.1	101	ARHVEHKKRQEEWEQ	KAT2B	1.413	1.343
AFH54221.1	101	ARHVEHKKRQEEWEQ	KAT5	1.094	0.71
AFH54221.1	253	KSEEFTRKVNRCSED	KAT2A	1.493	1.382

3.3. Forecasting transmembrane regions and subcellular localization of ROP13

According to TMHMM results, there observed one transmembrane domain in ROP13 sequence (Fig. 2). In addition, using the PSORT II program, ROP13 subcellular site was determined as follows: 33.3% plasma membrane, 22.2% endoplasmic reticulum, 33.3% Golgi, and 11.1% extracellular, including cell wall.

preprint

```
# AFH54221.1 Number of predicted TMHs:  1
# AFH54221.1 Exp number of AAs in TMHs: 20.38952
# AFH54221.1 Exp number, first 60 AAs:  16.79055
# AFH54221.1 Total prob of N-in:        0.84813
# AFH54221.1 POSSIBLE N-term signal sequence
# AFH54221.1      TMHMM2.0  inside        1   6
# AFH54221.1      TMHMM2.0  TMhelix       7   26
# AFH54221.1      TMHMM2.0  outside       27  400
```

A.

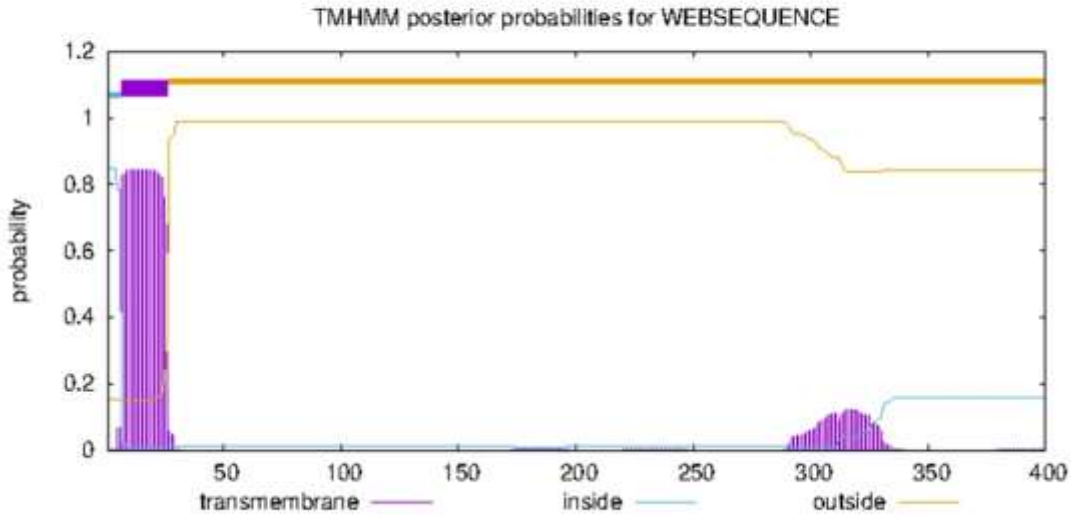

B.

Fig. 2. Bioinformatic analysis of the transmembrane domain of ROP13 sequence (http://www.cbs.dtu.dk/services/TMHMM-2.0/). (A) Number of predicted TMHs: The number of predicted transmembrane he- lices; Exp number of AAs in TMHs: The expected number of amino acids in- transmembrane helices. If this number is larger than 18 it is very likely to be a transmembrane protein (OR have a signal peptide); Exp number, first 60 AAs: The expected number of amino acids in transmembrane helices in the first 60 amino acids of the protein. If this number more than a few, you should be warned that a predicted transmembrane helix in the N-term could be a signal peptide; Total prob. of N-in: The total probability that the N-term is on the cytoplasmic side of the membrane; POSSIBLE N-term signal sequence: a warning that is produced when "Exp number, first 60 AAs" is larger than 10 (http://www.cbs.dtu.dk/services/TMHMM-2.0/TMHMM2.0.guide.html# output); (B) Graphical illustra- tion of transmembrane domain analysis of ROP13.

3.4. Assessment of secondary and tertiary structure

The GOR4 analysis showed that the secondary structure of the ROP13 protein consists of 400 amino acids and comprises 40% alpha helix (H) (160/400), 50.75% random coil (203/400), and 9.25% extended strand (37/400) (Fig. 3). The SWISS-MODEL findings are entirely depicted in Figure 4.

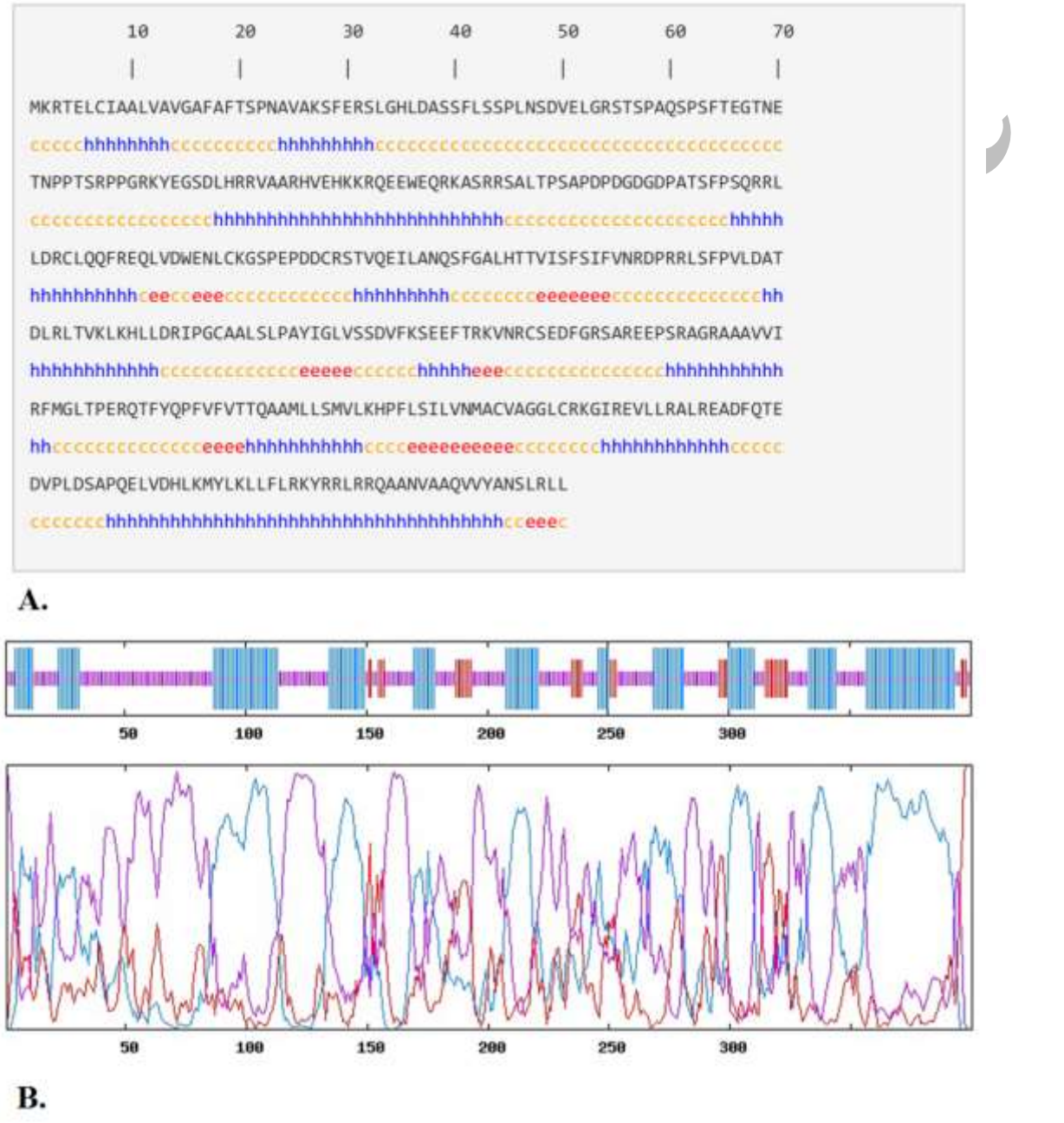

Fig. 3.

(A) Predicted secondary structure by GOR IV online service (https://npsa-prabi.ibcp.fr/cgi-bin/npsa_automat.pl?page=npsa_gor4.html). h = helix, e = ex- tended strand, and c = coil; (B) Graphical results for secondary structure prediction of ROP13 protein by GOR IV

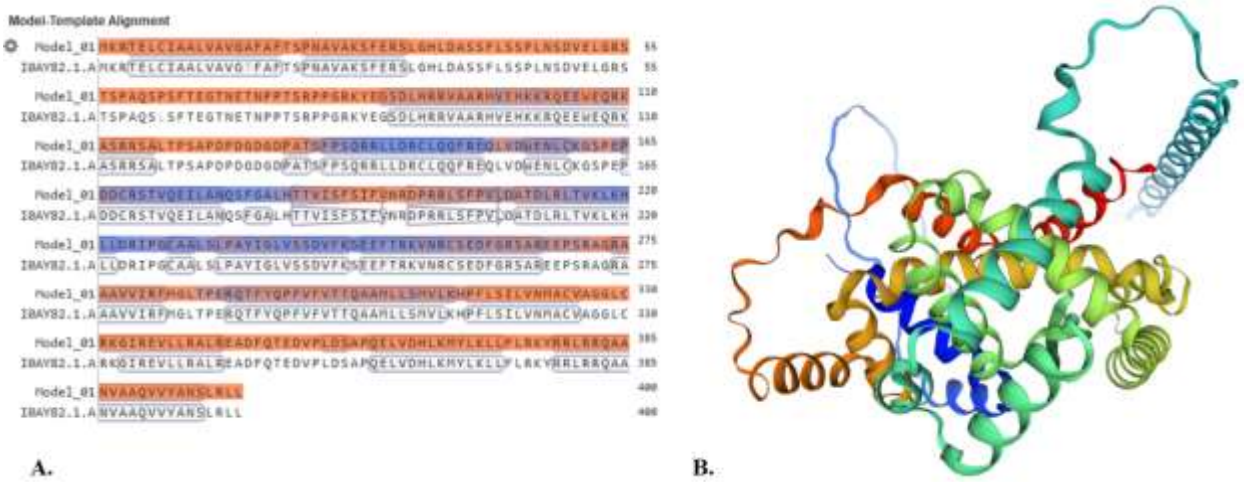

Fig. 4. Output of SWISS-MODEL, online server (https://swissmodel.expasy.org/).
(A) Sequence identity and) Model alignment; (B) The 3D model constructed for ROP13 protein

3.5. Verification the 3D model structure

The quality of the modeled structure was validated via representing the percentage of residues in disallowed and allowed areas (Fig. 5).

preprint

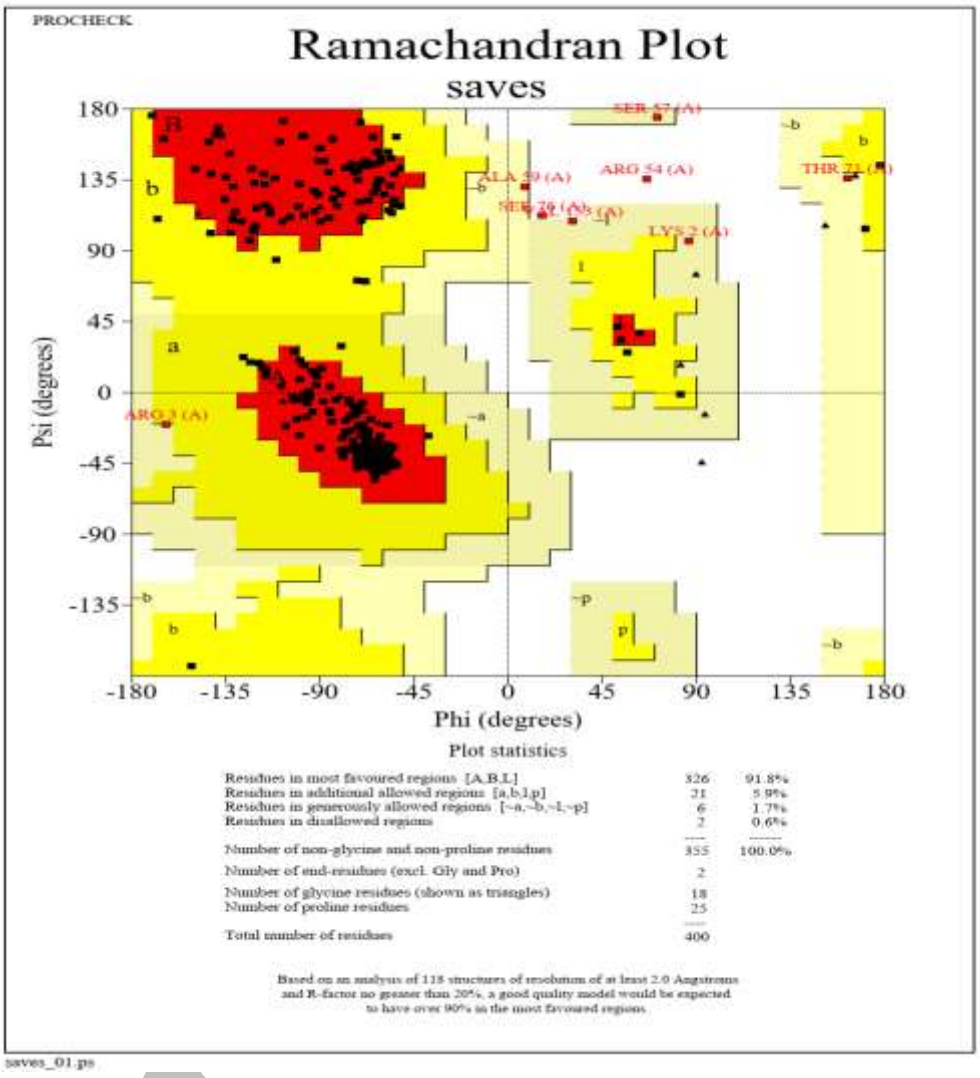

Fig. 5. ROP13 protein three-dimensional structure confirmation using the Ramachandran plot, available online at https://saves.mbi.ucla.edu/

The analysis of Ramachandran plot statistics revealed that 91.8% of amino acid residues from the structure modeled by SWISS-MODEL were incorporated in the favored regions; whereas only 7.6% and 0.6% are in allowed and disallowed regions of plot, respectively.

3.6. B-cell epitopes projection

Table 2 displays the results obtained from the Bcepred web server. Additionally, Table 3 presents the high-score 16-mer linear B-cell epitopes identified employing ABCpred. Only epitopes with a score higher than 0.75 are included in Table 3.

٢٩٥

٢٩٦ **Table 2.** Epitopes predicted in ROP13 protein by different parameters based on Bcepred online server

Prediction parameter	Epitope sequence
Flexibility	AVAKSFE; SFLSSPL; DVELGRSTS; PSFTEGTNETNPPTSRPPGRKYE; RHVEHKKRQEEWEQRKASRR; ENLCKGSPEPDDCR; IFVNRDP; EEFTRKVNRCSEDFGRSAREEPSRA; GLCRKGI; RKYRRLR
Hydrophilicity	GRSTSPAQSPS; TEGTNETNPPTSR; GRKYEGSD; EHKKRQEE; EQRKASRRSA; PSAPDPDGDGDPATS; CKGSPEPDDCRSTV; VNRCSEDFGRSAREEPSRAGR; ADFQTED
Accessibility	AKSFERSL; TSFPSQRRLLDR; LQQFREQL; KGSPEPDDCRST; FVNRDPRRLSFP; RSTSPAQSPSFTEGTNETNPPTSRPPGRKYEGSDLHRRVAARHVEHKKRQEEWEQRKAS RRSALTPSAPDPDGDGDP; DVFKSEEFTRKVNRCSE; FGRSAREEPSRAGR; GLTPERQTFYQP; CRKGIREV; RALREADFQTED; LFLRKYRRLRRQAANV;
Turns	-
Exposed Surface	-
Polarity	MKRTELCI; VAKSFERSLGHL; QRRLLDRC; PEPDDCRS; LCRKGIREVLLRALREAD; SRPPGRKYEGSDLHRRVAARHVEHKKRQEEWEQRKASRRSA; DPDGDGD; QRRLLDRC; VNRDPRRLS; RLTVKLKHLLDRI; DVFKSEEFTRKVNRCSE; FGRSAREEPSRAGR; ELVDHLKMYLKLLFLRKYRRLRRQAA;
Antigenic Propensity	SFLSSPL; RLLDRCLQQ; LHTTVISFSIFV; RLSFPVLD; LRLTVKLKHLL; YIGLVSSDVFK; TFYQPFVFVTTQ; MLLSMVLKHPFLSILVNM; GIREVLLR; QELVDHLKMYLKLLFLRKY

٢٩٧

٢٩٨ **Table 3.** Linear B-cell epitopes from full-length ROP13 protein using ABCpred server

Rank	Sequence	Start position	Score
1	VQEILANQSFGALHTT	172	0.91
2	SSDVFKSEEFTRKVNR	241	0.90
3	RRVAARHVEHKKRQEE	90	0.88
4	ENLCKGSPEPDDCRST	156	0.87
5	PSAPDPDGDGDPATSF	119	0.86
6	RRSALTPSAPDPDGDG	113	0.85
7	TNPPTSRPPGRKYEGS	71	0.83
7	TPERQTFYQPFVFVTT	286	0.83
7	AGRAAAVVIRFMGLTP	272	0.83

preprint

8	PAQSPSFTEGTNETNP	58	0.81
8	AVGAFAFTSPNAVAKS	13	0.81
8	DGDGDPATSFPSQRRL	125	0.81
8	EEWEQRKASRRSALTP	104	0.81
9	SFSIFVNRDPRRLSFP	190	0.79
10	RPPGRKYEGSDLHRRV	77	0.78
11	LFLRKYRRLRRQAANV	372	0.75
11	LPAYIGLVSSDVFKSE	233	0.75
12	PQELVDHLKMYLKLLF	358	0.74
12	PGCAALSLPAYIGLVS	226	0.74
12	SFPSQRRLLDRCLQQF	133	0.74
13	YEGSDLHRRVAARHVE	83	0.73
13	ALREADFQTEDVPLDS	341	0.73
14	RSAREEPSRAGRAAAV	263	0.71
14	QFREQLVDWENLCKGS	147	0.71
15	TVKLKHLLDRIPGCAA	215	0.70
16	GGLCRKGIREVLLRAL	327	0.69
17	LGHLDASSFLSSPLNS	33	0.68
18	SSFLSSPLNSDVELGR	39	0.67
18	LSMVLKHPFLSILVNM	307	0.67
19	ELCIAALVAVGAFAFT	5	0.66
19	SDVELGRSTSPAQSPS	48	0.66
19	SILVNMACVAGGLCRK	317	0.66
20	NRDPRRLSFPVLDATD	196	0.65
21	VTTQAAMLLSMVLKHP	299	0.61

preprint

22	RLRRQAANVAAQVVYA	379	0.60
23	FPVLDATDLRLTVKLK	204	0.59
24	YQPFVFVTTQAAMLLS	293	0.58
25	NAVAKSFERSLGHLDA	23	0.52

٢٩٩ The graphical prediction of continuous B-cell epitopes for ROP13 was conducted using the
٣٠٠ following threshold values for different parameters: Bepipred linear (0.502), hydrophilicity
٣٠١ (1.471), flexibility (1.000), antigenicity (1.038), beta-turn (0.966), and surface accessibility
٣٠٢ (1.000) (Fig. 6). Fourteen discontinuous epitopes of B-cell were forecasted employing the ElliPro
٣٠٣ server (Table 4).

٣٠٤ **Table 4.** Conformational B cell epitopes of TgROP13 protein predicted by ElliPro server.

No.	Residues	Number of Residues	Score	3D structure
1	A:R77, A:P78, A:P79, A:G80, A:R81 (RPPGR)	5	0.958	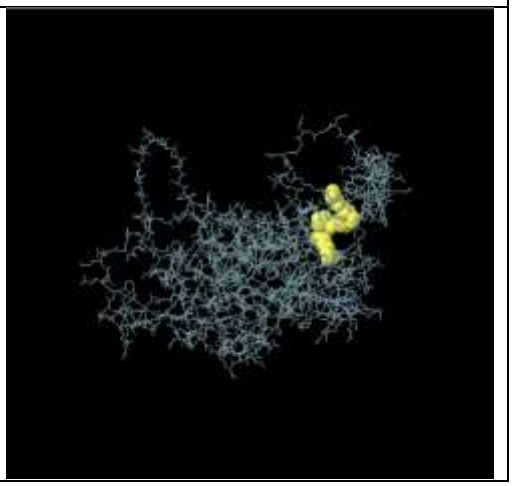

preprint

2	A:L42, A:S43, A:S44, A:P45, A:L46, A:N47, A:S48, A:D49, A:V50, A:E51, A:L52, A:G53, A:R54, A:S55, A:T56, A:S57, A:P58, A:A59, A:Q60, A:S61, A:P62, A:S63, A:F64, A:T65, A:E66, A:G67, A:T68, A:N69, A:E70, A:T71, A:N72, A:P73, A:P74, A:T75, A:S76 (LSSPLNSDVELGRSTSPAQSPSFTEGTNETNPPTS)	35	0.921	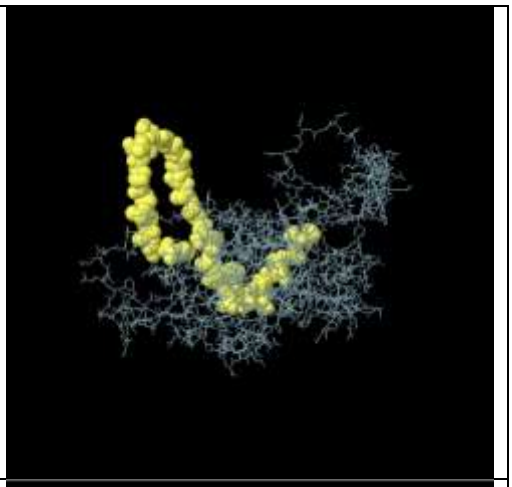
3	A:E84, A:G85, A:S86, A:D87, A:L88, A:H89, A:R90, A:R91 (EGSDLHRR)	8	0.893	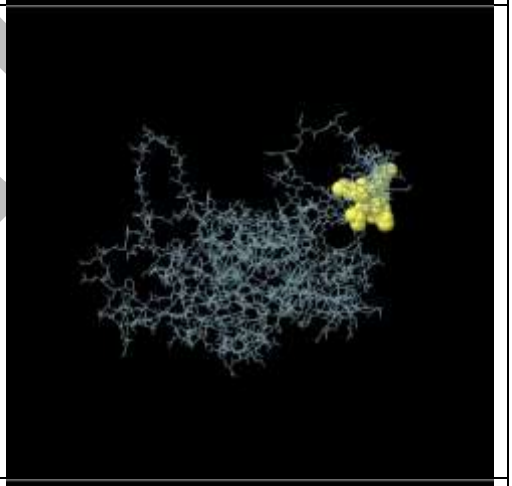
4	A:V92, A:A93, A:A94, A:R95, A:H96, A:V97, A:E98, A:H99, A:K100, A:K101, A:R102, A:Q103, A:E104, A:E105, A:W106, A:R109 (VAARHVEHKKRQEEWR)	16	0.779	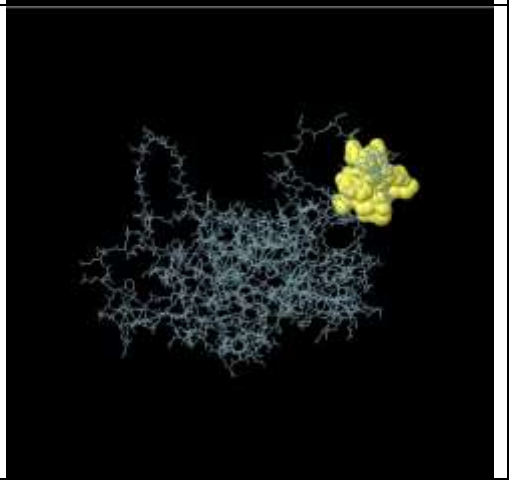

Preprint

5	A:E107, A:K110, A:A111, A:S112, A:R113, A:R114, A:S115, A:A116, A:L117, A:T118, A:P119, A:S120, A:A121, A:P122, A:D123, A:P124, A:D125, A:G126, A:D127, A:G128, A:D129, A:P130, A:A131, A:T132, A:S133, A:P135, A:S136, A:R139 (EKASRRSALTPSAPDPDGDG DPATSPSR)	28	0.773	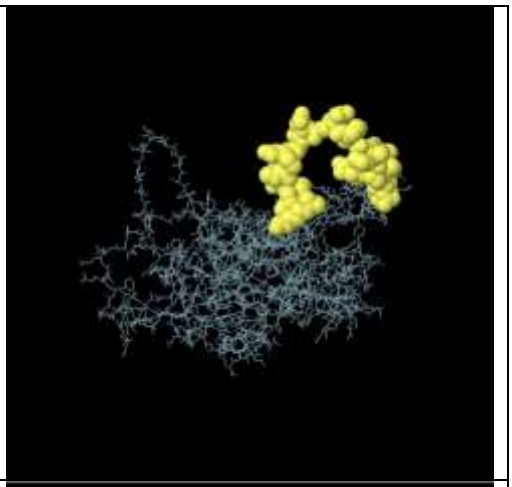
6	A:L36, A:D37, A:A38, A:S39, A:S40, A:F41 (LDASSF)	6	0.742	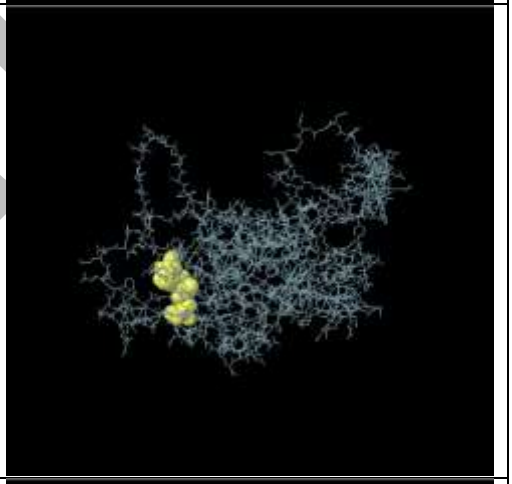
7	A:Q348, A:T349, A:E350, A:D351, A:V352, A:P353, A:L354, A:D355, A:S356, A:A357 (QTEDVPLDSA)	10	0.708	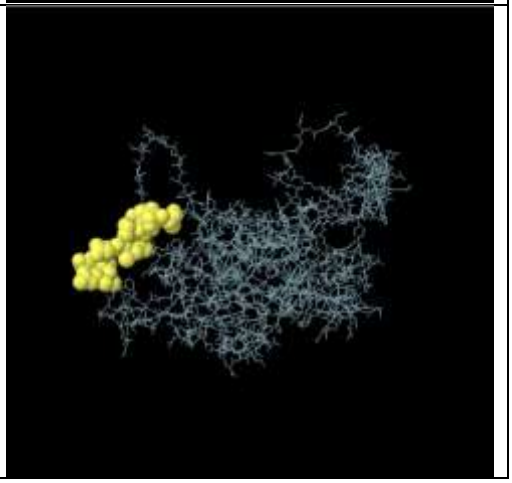

prepri

8	A:A326, A:G327, A:G328, A:L329, A:C330, A:G333, A:I334, A:R335, A:E336, A:V337, A:L338, A:L339, A:R340, A:A341, A:L342, A:R343, A:E344, A:A345, A:D346, A:F347 (AGGLCGIREVLLRALREADF)	20	0.679	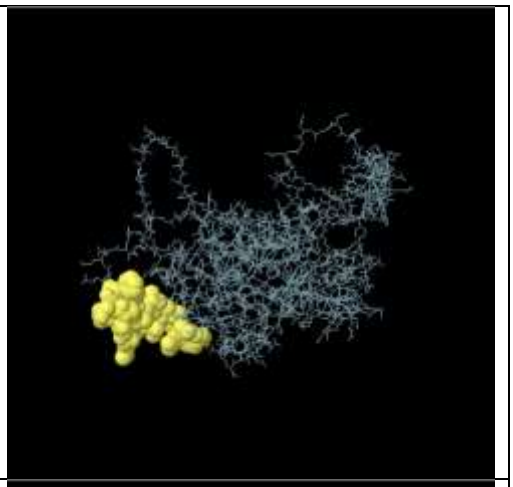
9	A:S21, A:N23, A:A24, A:A26, A:K27, A:S28, A:F29, A:E30, A:R31, A:S32, A:L33, A:G34, A:H35 (SNAAKSFERSLGH)	13	0.648	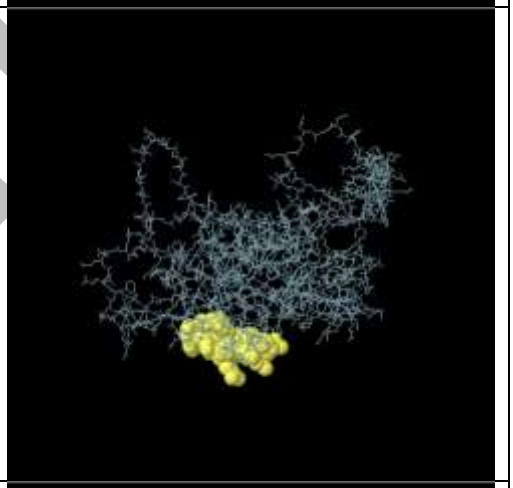
10	A:F148, A:L152, A:V153, A:D154, A:W155, A:E156, A:N157, A:K160, A:G161, A:S162, A:P163, A:E164, A:P165, A:D166, A:D167, A:R169, A:S170, A:Q173 (FLVDWENKGSPEPDDRSQ)	18	0.589	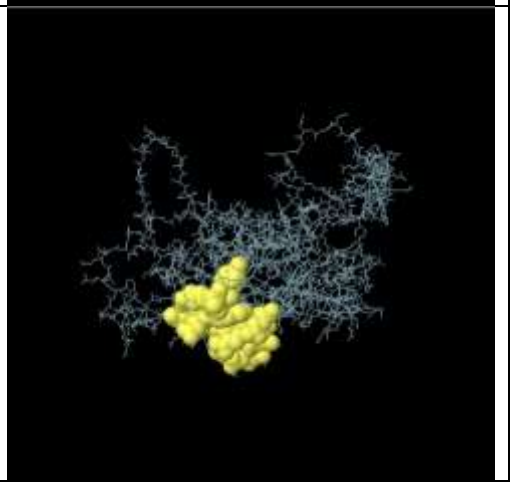

Preprint

11	A:L140, A:D142, A:R143, A:C144, A:L145, A:Q146, A:Q147, A:R149, A:E150, A:Q151, A:E174, A:L176, A:A177, A:N178, A:Q179, A:S180, A:A183, A:D223, A:I225, A:P226, A:G227, A:C228, A:A229, A:A230, A:L231 (LDRCLQQREQELANQSADIP GCAAL)	25	0.581	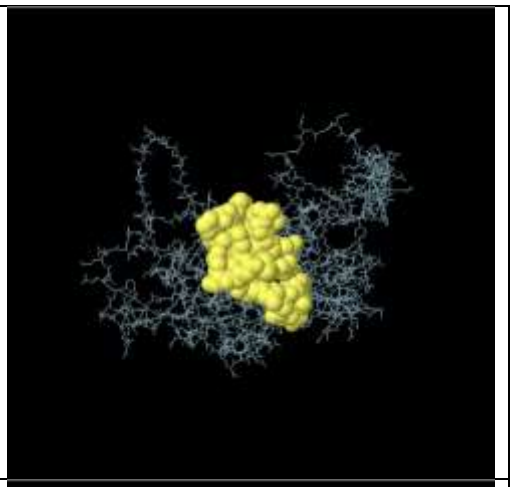
12	A:E259, A:G262, A:R263, A:A265, A:R266, A:E267, A:R281 (EGRARER)	7	0.559	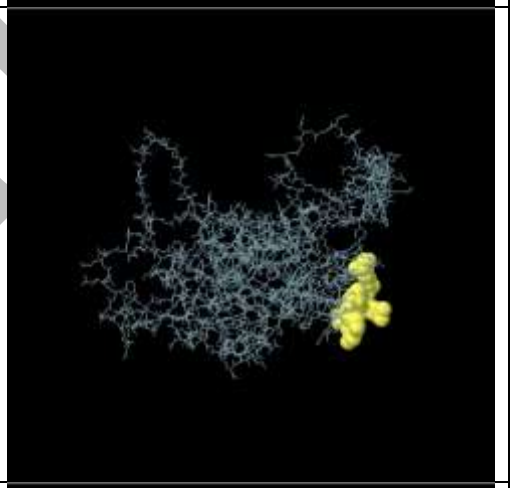
13	A:E268, A:P269, A:S270, A:A272, A:G273, A:R274 (EPSAGR)	6	0.516	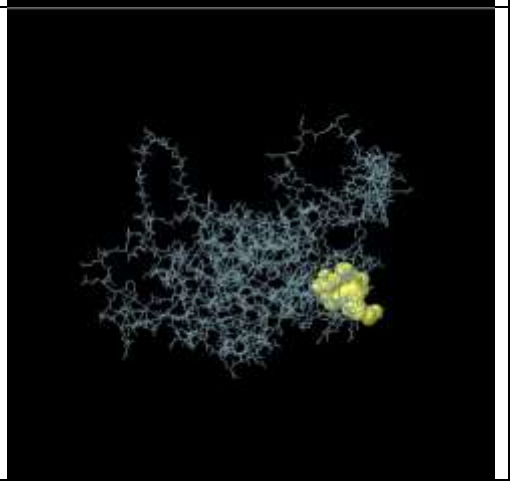

prepri

14	A:G284, A:L285, A:T286 (GLT)	3	0.505	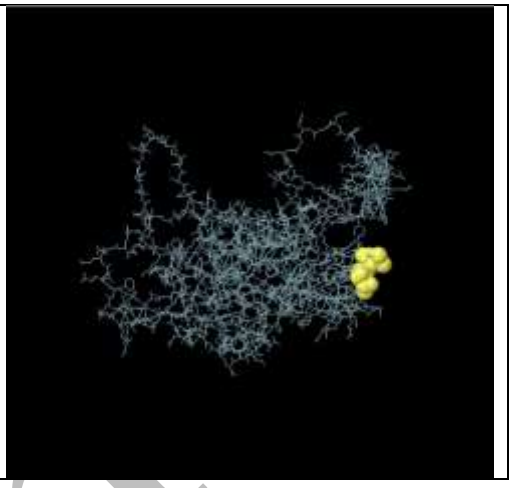

preprint

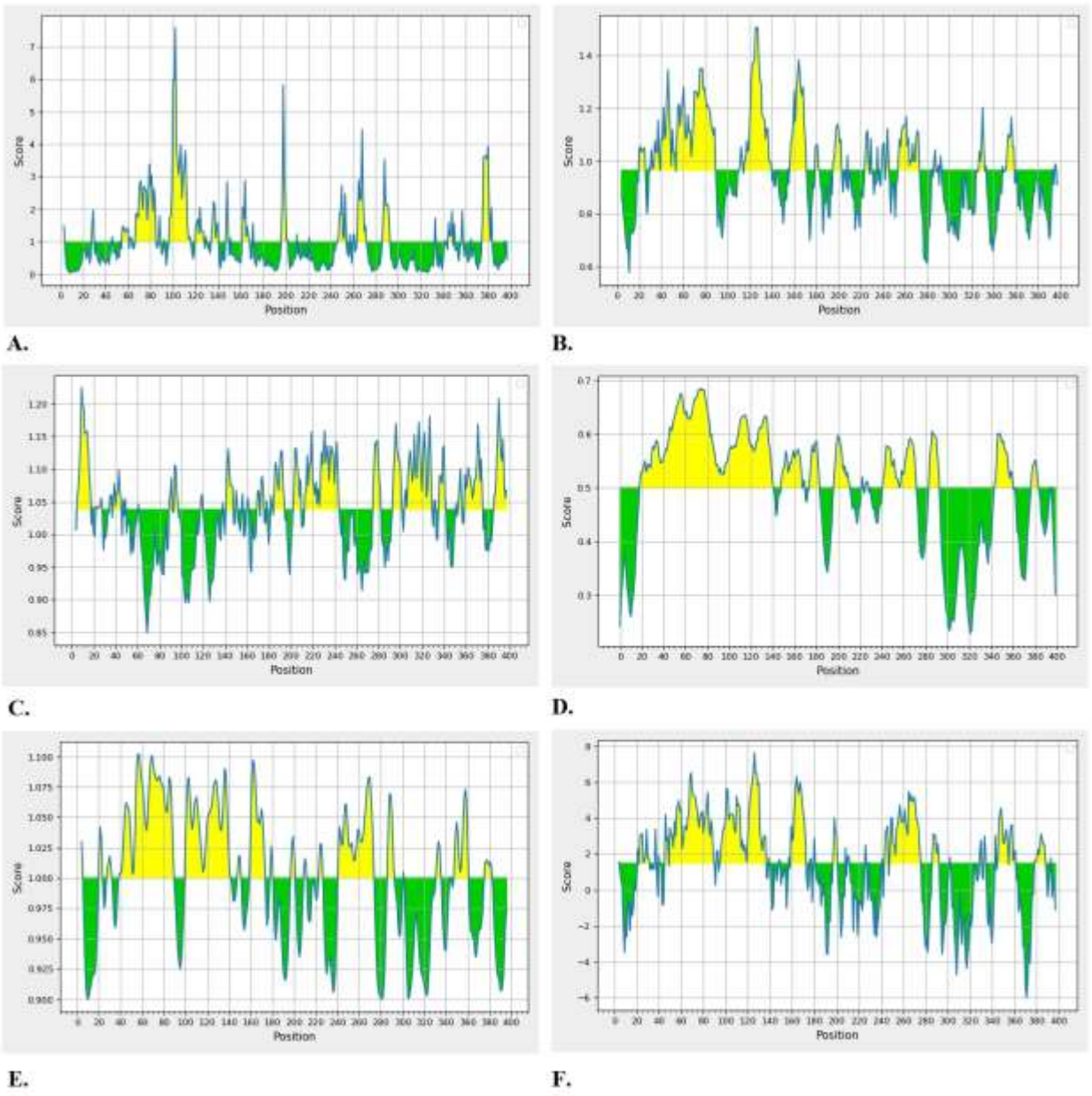

Fig. 6. Linear B-cell epitopes of ROP13 protein sequence predicted by ProtScale server (https://web.expasy.org/protscale/), based on percent of accessible residues(A), Beta-turn (B), Antigenicity (C), Bepipred linear (D), Flexibility (E) and Hydrophilicity (F). The horizontal line indicates the threshold or the average score. Yellow colors (above the threshold) indicate favorable regions related to the properties of interest. Green color (below the threshold) indicates the unfavorable regions related to the properties of interest.

3.7. MHC-I and MHC-II binding epitopes projection

The T-cell epitopes with the lowest IC_{50} values (or percentile ranks) were selected. The minimum percentile scores of each MHC allele for ROP13 are presented in Table 5 and 6.

Table 5. IC_{50} values for ROP13 binding to MHC class I molecules obtained using the IEDB[a].

MHC I allele[a]	Start-Stop[c] ROP13	Peptide sequence	Percentile rank[d] ROP13
H2-Db	43-52	SSPLNSDVEL	0.165
H2-Db	6-15	SAPQELVDHL	0.4
H2-Db	18-27	CAALSLPAYI	0.44
H2-Dd	57-66	RDPRRLSFPV	0.545
H2-Dd	7-16	RPPGRKYEGS	1.4
H2-Dd	5-14	LTPERQTFYQ	1.8
H2-Kb	41-50	VVYANSLRLL	0.355
H2-Kb	27-36	KSFERSLGHL	0.47
H2-Kb	10-19	QTFYQPFVFV	2.2
H2-Kd	27-34	AYIGLVSSDV	0.35
H2-Kd	39-48	QSFGALHTTV	2.85
H2-Kd	26-35	KYRRLRRQAA	3.35
H2-Kk	34-43	EEWEQRKASR	7.65
H2-Kk	21-30	TQAAMLLSMV	9.2
H2-Kk	28-37	SFERSLGHLD	10.8
H2-Ld	33-42	HPFLSILVNM	0.74
H2-Ld	14-23	RIPGCAALSL	2.6
H2-Ld	2-11	VPLDSAPQEL	2.7

[a]The immune epitope database (http://tools.iedb.org/mhci/). [b]H2-Db, H2-Dd, H2-Kb, H2-Kd, H2-Kk, and H2-Ld alleles are mouse MHC class I molecules. [c]Ten amino acids for analysis were used each time. [d]Low percentile rank = high level binding; high percentile rank = low level binding; IC_{50} values = percentile rank.

preprint

٣٣٠ **Table 6.** IC_{50} values for ROP13 binding to MHC class II molecules obtained using the IEDB[a].

MHC II allele[b]	Start-Stop[c] ROP13	Peptide sequence	Percentile rank[d] ROP13
H2-IAb	13-27	AVGAFAFTSPNAVAK	0.01
H2-IAb	15-29	GAFAFTSPNAVAKSF	0.01
H2-IAb	36-50	LDASSFLSSPLNSDV	1.96
H2-IAd	4-18	TELCIAALVAVGAFA	1.23
H2-IAd	6-20	LCIAALVAVGAFAFT	1.8
H2-IAd	30-44	LRRQAANVAAQVVYA	2.27
H2-IEd	20-34	KLLFLRKYRRLRRQA	0.05
H2-IEd	17-31	MYLKLLFLRKYRRLR	0.15
H2-IEd	24-38	LRKYRRLRRQAANVA	1.09

٣٣١ [a]The immune epitope database (http://tools.immuneepitope.org/mhcii). [b]H2-IAb, H2-IAd, and H2-IEd alleles are
٣٣٢ mouse MHC class II molecules. [c]Fifteen amino acids for analysis were used each time. [d]Low percentile rank = high
٣٣٣ level binding; high percentile rank = low level binding; IC_{50} values = percentile rank.

٣٣٤ ## 3.8. CTL epitope projection

٣٣٥ The ten high ranked CTL epitopes of the ROP13 protein were identified and presented in Table 7.

٣٣٦ **Table 7.** Predicted ROP13 epitopes by CTLpred[a].

Peptide rank	Start position[b]	Sequence	Score (ANN/SVM)[c]	Prediction
1	258	SEDFGRSAR	0.99/0.91	Epitope
2	223	DRIPGCAAL	0.43/1.28	Epitope
3	217	KLKHLLDRI	0.90/0.76	Epitope
4	133	SFPSQRRLL	0.97/0.65	Epitope
5	253	KVNRCSEDF	0.96/0.61	Epitope
6	374	LRKYRRLRR	0.67/0.85	Epitope
7	187	TVISFSIFV	0.51/1.00	Epitope
8	132	TSFPSQRRL	0.44/1.05	Epitope
9	277	AVVIRFMGL	0.04/1.44	Epitope
10	334	IREVLLRAL	0.24/1.23	Epitope

٣٣٧ [a]CTLpred, available online at http://www.imtech.res.in/raghava/ctlpred/index.html. [b]Nine amino acids for analysis
٣٣٨ were used. [c]The default artificial neural network (ANN) and support vector machine (SVM) cut-off scores were set
٣٣٩ 0.51 and 0.36, respectively.

٣٤٠

٣٤١ ## 3.9. Antigenicity, allergenicity, and solubility assessment

٣٤٢ The antigenicity scores of ROP13 were calculated as 0.821125 and 0.5796 using ANTIGEN¬pro
٣٤٣ and VaxiJen v.2.0, respectively. A threshold value of 0.5 was considered for both models.

preprint

The findings of the AlgPred server using the hybrid approach demonstrated that the ROP13 protein is not allergen.

The ROP13 protein solubility after overexpression in *E. coli* was calculated at 0.7847.

4. Discussion

Toxoplasmosis is now widely remained as one of the main threat to human society and livestock industry that lacks a global solution (6,7,13). So far, no vaccine or appropriate treatment is available to prevent and control of this infectious disease. Furthermore, the existing drugs are not entirely satisfactory and can induce adverse side effects in patients (7,14). Hence, the quest to develop an effective and safe vaccine specifically targeting toxoplasmosis has been a key area of research for scientists worldwide (43).

Nevertheless, designing successful vaccines with conventional methods is expensive, tedious, and takes considerable time. *In silico* is the most successful technology to the identification of accurate biomarkers to guide treatment selection that can significantly reduce both time and cost of diagnosis (44). Research has demonstrated that the ROP family has a critical impact on invasion of *T. gondii* and its interaction with host cells (20,21). The ROP13 protein has the ability to enter the cytoplasm of host cells, demonstrating strong immunogenicity and pathogenicity (22). Current investigation was performed to analyze and compare the different aspects of the ROP13 protein using bioinformatics techniques and online servers to design a suitable toxoplasmosis vaccine. The present research employed multiple bioinformatic tools to assess the diverse features of ROP13. It is indicated that peptides with MW of < 5–10 KDa are regarded as a poor immunogenic (45). Herein, it has been found that the amino acid sequence of the ROP13 protein comprises 400 residues and an average MW of 44,714.15 D, suggesting a good antigenic nature.

Our analysis showed that the aliphatic index and GRAVY score of the ROP13 sequence were calculated as 84.40 and -0.311, respectively. A high aliphatic index shows that the target protein is stable over a broad spectrum of temperatures. The negative or low GRAVY score highlights that the peptide has better interaction with surrounding water molecules. It is widely recognized that ROPs contain an N-terminal signal sequence and a C-terminal hydrophobic sequence, which is believed to include a transmembrane region (46).

preprint

In this study, we observed that there was only one transmembrane region for ROP13 gene sequence. Studies have indicated that PTM sites serve as a set of enzymatic functions capable of modulating the function, structure, and stability of proteins (47). Accordingly, we identified acylation and phosphorylation sites on the ROP13 protein. Our findings revealed a total of 43 PTM sites (2 acylation and 41 phosphorylation positions) within the sequence. These sites suggest the potential modulation of protein function, which could influence its activity.

It is well established that the secondary structure of proteins depends on the hydrogen bond pattern between amino hydrogen atoms and carboxyl oxygen atoms in a polypeptide chain, with alpha helices and beta sheets being the commonest structure (48). Proteins play a crucial role in the body due to their three-dimensional shape. Understanding the correlation between protein structure and function is essential. Therefore, determining the tertiary structure of proteins is a key step in unraveling their functional properties (47). Our investigation into the secondary structure of ROP13 revealed that it contains 40% alpha helix, 9.25% extended strand, and 50.75% random coil. The plot of Ramachandran revealed that 91.8% of amino acid residues were located in the ideal regions, with 7.6% and 0.6% found in the allowed and disallowed regions of the plot, respectively.

Several studies have demonstrated that immunization against *T. gondii* infection is conferred through acquired immune responses, including humoral and cellular immunity, as well as regulatory cytokines (48–52). Specific IgG antibodies, acting as anti-*Toxoplasma* antibodies, effectively control and limit parasite growth (50). They interfere parasite replication by limiting its adhesion to surface receptors on host cells and inhibiting with the functions of parasite proteins (50,51). They also stimulate macrophage phagocytosis, which enhances the body's immune response against intracellular parasite infections (51,52). Additionally, the secretion of interferon-γ (IFN-γ) by CD4+ and CD8+ T-cells is a critical indicator of cellular response generation. This response is essential for preventing the reactivation of bradyzoites within the host tissue cyst (51,52). In addition, epitope identification is helpful as it directly induce a robust immunity to properly control the parasite in vaccine design researches (47). *In silico* B-cell epitope mapping enables a better understanding of epitopes that are essential with regards to the interactions that happen between antibodies and pathogens.

preprint

The continuous B-cell epitope prediction results revealed that the ROP13 protein contains positive epitopes with acceptable indexes, as determined using the Bcepred online server. Subsequently, we utilized this server to identify B-cell epitopes based on various physicochemical characteristics including accessibility, hydrophilicity, flexibility/mobility, exposed surface, polarity, turns, or a combination of these properties (19).

The lower IC_{50} values indicate a higher affinity for MHC binding, indicating an appropriate T-cell epitope. The analysis of IC_{50} values of peptides from the IEDB output indicated that the T-cell epitopes on ROP13 can strongly bind to MHC class I and class II molecules.

5. Conclusion

This research provides insights into the potential role of the ROP13 protein in combating *T. gondii* infection, supported by bioinformatics analyses. However, further experimental validation is needed to definitively assess its effectiveness. The goal of such studies is to completely comprehend the role of the ROP13 proteins in preventing *T. gondii* infection, which requires conducting comprehensive experimental studies and finding more information.

Declarations

Acknowledgement

We sincerely thank personnel from the Medical Microbiology Research Center, Qazvin University of Medical Sciences, Qazvin, Iran and Jahrom University of Medical Sciences, Jahrom, Iran.

Author contribution

MB, AVE, MF and LZ designed the study. MB, MGC, AKS, DD, and MP searched for primary publications, screened and appraised of data. MB, LZ and AVE wrote the study manuscript. MB, KHN and AVE: edited the manuscript. DD, MB, AVE and MF contributed to data analysis. All authors read the manuscript and participated in the preparation of the final version of the manuscript.

Competing interests

preprint

The authors declared no potential conflicts of interest concerning the research or authorship.

Funding

This work was supported by the Medical Microbiology Research Center, Qazvin University of Medical Sciences, Qazvin, Iran (contract no. IR.QUMS.REC.1400.481). The funder of the study had no role in study design, data collection, data analysis, data interpretation, or writing of the report.

Ethics approval and consent to participate

The current study was performed by approval of the ethics committee of Qazvin Medical University with approval number IR.QUMS.REC.1400.481. The research protocol was approved by the Research Ethics Committee at the Qazvin Medical University, Iran.

Consent for publication

Not applicable

Availability of data and materials

The datasets used and/or analyzed during the current study are available from the corresponding author on reasonable request.

List of abbreviations

ROP13: Rhoptry Protein 13, NCBI: National Center for Biotechnology Information, GRAVY: grand average of hydropathicity, CTL: Cytotoxic T lymphocyte, PI: protusion index, GOR: Garnier-Osguthorpe-Robson

References

preprint

1. Rostami A, Riahi SM, Gamble HR, Fakhri Y, Shiadeh MN, Danesh M, et al. Global prevalence of latent toxoplasmosis in pregnant women: a systematic review and meta-analysis. Clin Microbiol Infect. 2020;26(6):673–83.
2. Abbasali Z, Pirestani M, Dalimi A, Badri M, Fasihi-Ramandi M. Anti-parasitic activity of a chimeric peptide Cecropin A (2- 8)-Melittin (6- 9)(CM11) against tachyzoites of *Toxoplasma gondii* and the BALB/c mouse model of acute toxoplasmosis. Mol Biochem Parasitol. 2023;255:111578.
3. Bohne W, Gross U, Ferguson DJP, Heesemann J. Cloning and characterization of a bradyzoite-specifically expressed gene (hsp30/bag1) of *Toxoplasma gondii*, related to genes encoding small heat-shock proteins of plants. Mol Microbiol. 1995;16(6):1221–30.
4. Sanchez SG, Besteiro S. The pathogenicity and virulence of *Toxoplasma gondii*. Virulence. 2021;12(1):3095–114.
5. Haghbin M, Maani S, Bagherzadeh MA, Bazmjoo A, Shakeri H, Taghipour A, et al. Latent Toxoplasmosis among Breast Cancer Patients in Jahrom, South of Iran. Int J Breast Cancer. 2023;2023.
6. Dubey JP. The history of *Toxoplasma gondii* the first 100 years. J Eukaryot Microbiol. 2008;55(6):467–75.
7. Wang ZD, Liu HH, Ma ZX, Ma HY, Li ZY, Yang ZB, et al. *Toxoplasma gondii* infection in immunocompromised patients: a systematic review and meta-analysis. Front Microbiol. 2017;8:238621.
8. Mose JM, Kagira JM, Kamau DM, Maina NW, Ngotho M, Karanja SM, et al. A review on the present advances on studies of toxoplasmosis in eastern Africa. Biomed Res Int. 2020;2020.
9. Dupont CD, Christian DA, Hunter CA. Immune response and immunopathology during toxoplasmosis. In: Seminars in immunopathology. 2012. p. 793–813.
10. Abdoli A, Olfatifar M, Eslahi AV, Moghadamizad Z, Samimi R, Habibi MA, et al. A systematic review and meta-analysis of protozoan parasite infections among patients with mental health disorders: an overlooked phenomenon. Gut Pathog. 2024;16(1):7.
11. Gharavi MJ, Jalali S, Khademvatan S, Heydari S. Detection of IgM and IgG anti-*Toxoplasma* antibodies in renal transplant recipients using ELFA, ELISA and ISAGA

preprint

methods: comparison of pre-and post-transplantation status. Ann Trop Med & Parasitol. 2011;105(5):367–71.

12. Weiss LM, Dubey JP. Toxoplasmosis: A history of clinical observations. Int J Parasitol. 2009;39(8):895–901.

13. Tenter AM. *Toxoplasma gondii* in animals used for human consumption. Mem Inst Oswaldo Cruz. 2009;104:364–9.

14. Hajj R El, Tawk L, Itani S, Hamie M, Ezzeddine J, El Sabban M, et al. Toxoplasmosis: Current and emerging parasite druggable targets. Microorganisms. 2021;9(12):2531.

15. Antczak M, Dzitko K, Dugoska H. Human toxoplasmosis Searching for novel chemotherapeutics. Biomed Pharmacother. 2016;82:677–84.

16. Pagheh AS, Sarvi S, Sharif M, Rezaei F, Ahmadpour E, Dodangeh S, et al. *Toxoplasma gondii* surface antigen 1 (SAG1) as a potential candidate to develop vaccine against toxoplasmosis: A systematic review. Comp Immunol Microbiol Infect Dis. 2020;69:101414.

17. Zhang NZ, Chen J, Wang M, Petersen E, Zhu XQ. Vaccines against *Toxoplasma gondii*: new developments and perspectives. Expert Rev Vaccines. 2013;12(11):1287–99.

18. Rezaei F, Sarvi S, Sharif M, Hejazi SH, sattar Pagheh A, Aghayan SA, et al. A systematic review of *Toxoplasma gondii* antigens to find the best vaccine candidates for immunization. Microb Pathog. 2019;126:172–84.

19. Kazi A, Chuah C, Majeed ABA, Leow CH, Lim BH, Leow CY. Current progress of immunoinformatics approach harnessed for cellular-and antibody-dependent vaccine design. Pathog Glob Health. 2018;112(3):123–31.

20. Dlugonska H, others. Toxoplasma rhoptries: unique secretory organelles and source of promising vaccine proteins for immunoprevention of toxoplasmosis. Biomed Res Int. 2008;2008.

21. Pagheh AS, Daryani A, Alizadeh P, Hassannia H, Oliveira SMR, Kazemi T, et al. Protective effect of a DNA vaccine cocktail encoding ROP13 and GRA14 with Alum nano-adjuvant against *Toxoplasma gondii* infection in mice. Int J Biochem & Cell Biol. 2021;132:105920.

22. Turetzky JM, Chu DK, Hajagos BE, Bradley PJ. Processing and secretion of ROP13: A unique *Toxoplasma* effector protein. Int J Parasitol. 2010;40(9):1037–44.

preprint

23. Wang PY, Yuan ZG, Petersen E, Li J, Zhang XX, Li XZ, et al. Protective efficacy of a *Toxoplasma gondii* rhoptry protein 13 plasmid DNA vaccine in mice. Clin Vaccine Immunol. 2012;19(12):1916–20.

24. Kang HJ, Lee SH, Kim MJ, Chu KB, Lee DH, Chopra M, et al. Influenza virus-like particles presenting both *Toxoplasma gondii* ROP4 and ROP13 Enhance Protection against T. gondii infection. Pharmaceutics. 2019;11(7):342.

25. Zhou J, Wang L, Zhou A, Lu G, Li Q, Wang Z, et al. Bioinformatics analysis and expression of a novel protein ROP48 in *Toxoplasma gondii*. Acta Parasitol. 2016;61(2):319–28.

26. Romano P, Giugno R, Pulvirenti A. Tools and collaborative environments for bioinformatics research. Brief Bioinform. 2011;12(6):549–61.

27. Gasteiger E, Hoogland C, Gattiker A, Duvaud S, Wilkins MR, Appel RD, et al. Protein identification and analysis tools on the ExPASy server. Springer; 2005.

28. Garnier J, Gibrat JF, Robson B. GOR method for predicting protein secondary structure from amino acid sequence. In: Methods in enzymology. Elsevier; 1996. p. 540–53.

29. Guex N, Peitsch MC, Schwede T. Automated comparative protein structure modeling with SWISS-MODEL and Swiss-PdbViewer: A historical perspective. Electrophoresis. 2009;30(S1):S162--S173.

30. Colovos C, Yeates TO. Verification of protein structures: patterns of nonbonded atomic interactions. Protein Sci. 1993;2(9):1511–9.

31. Saha S, Raghava GPS. Prediction of continuous B-cell epitopes in an antigen using recurrent neural network. Proteins Struct Funct Bioinforma. 2006;65(1):40–8.

32. Saha S, Raghava GPS. BcePred: prediction of continuous B-cell epitopes in antigenic sequences using physico-chemical properties. In: International conference on artificial immune systems. 2004. p. 197–204.

33. Ponomarenko J, Bui HH, Li W, Fusseder N, Bourne PE, Sette A, et al. ElliPro: a new structure-based tool for the prediction of antibody epitopes. BMC Bioinformatics. 2008;9:1–8.

34. Wang P, Sidney J, Dow C, Mothé B, Sette A, Peters B. A systematic assessment of MHC class II peptide binding predictions and evaluation of a consensus approach. PLoS Comput Biol. 2008;4(4):e1000048.

preprint

٥٣٩ 35. Wang P, Sidney J, Kim Y, Sette A, Lund O, Nielsen M, et al. Peptide binding predictions
٥٤٠ for HLA DR, DP and DQ molecules. BMC Bioinformatics. 2010;11:1–12.
٥٤١ 36. Bhasin M, Raghava GPS. Prediction of CTL epitopes using QM, SVM and ANN
٥٤٢ techniques. Vaccine. 2004;22(23–24):3195–204.
٥٤٣ 37. Magnan CN, Zeller M, Kayala MA, Vigil A, Randall A, Felgner PL, et al. High-
٥٤٤ throughput prediction of protein antigenicity using protein microarray data.
٥٤٥ Bioinformatics. 2010;26(23):2936–43.
٥٤٦ 38. Doytchinova IA, VaxiJen DRF. A server for prediction of protective antigens, tumour
٥٤٧ antigens and subunit vaccines., 2007, 8, 4. DOI https//doi org/101186/1471-2105-8-4.
٥٤٨ 39. Saha S, Raghava GPS. AlgPred: prediction of allergenic proteins and mapping of IgE
٥٤٩ epitopes. Nucleic Acids Res. 2006;34(suppl_2):W202–9.
٥٥٠ 40. Magnan CN, Randall A, Baldi P. SOLpro: accurate sequence-based prediction of protein
٥٥١ solubility. Bioinformatics. 2009;25(17):2200–7.
٥٥٢ 41. Kur J, Holec-G\kasior L, Hiszczyńska-Sawicka E. Current status of toxoplasmosis vaccine
٥٥٣ development. Expert Rev Vaccines. 2009;8(6):791–808.
٥٥٤ 42. Dodangeh S, Fasihi-Ramandi M, Daryani A, Valadan R, Sarvi S. In silico analysis and
٥٥٥ expression of a novel chimeric antigen as a vaccine candidate against *Toxoplasma gondii*.
٥٥٦ Microb Pathog. 2019;132:275–81.
٥٥٧ 43. Berzofsky JA. Immunogenicity and antigen structure. Fundam Immunol Third ed.
٥٥٨ 1993;235–82.
٥٥٩ 44. El Hajj H, Demey E, Poncet J. The ROP2 family of *Toxoplasma gondii* rhoptry proteins:
٥٦٠ proteomic and genomic characterization and molecular modeling.
٥٦١ 45. Walsh C. Posttranslational modification of proteins: expanding nature's inventory.
٥٦٢ Roberts and Company Publishers; 2006.
٥٦٣ 46. Yada RY, Jackman RL, Nakai S. Secondary structure prediction and determination of
٥٦٤ proteins a review. Int J Pept Protein Res. 1988;31(1):98–108.
٥٦٥ 47. Wang Y, Wang G, Cai J, Yin H. Review on the identification and role of *Toxoplasma*
٥٦٦ *gondii* antigenic epitopes. Parasitol Res. 2016;115:459–68.
٥٦٧ 48. Zaki L, Ghaffarifar F, Sharifi Z, Horton J, Sadraei J. Effect of Imiquimod on Tachyzoites
٥٦٨ of *Toxoplasma gondii* and Infected Macrophages in vitro and in BALB/c Mice. Front Cell
٥٦٩ Infect Microbiol. 2020;10:387.

preprint

٥٧٠ 49. Zaki L, Ghaffarifar F, Sharifi Z, Horton J, Sadraei J. *Toxoplasma gondii*: preventive and
٥٧١ therapeutic effects of morphine and evaluation of treatment parameters of tachyzoites and
٥٧٢ infected macrophages in vitro and in a murine model. EXCLI J. 2020;19:514.
٥٧٣ 50. Sayles PC, Gibson GW, Johnson LL. B cells are essential for vaccination-induced
٥٧٤ resistance to virulent *Toxoplasma gondii*. Infect Immun. 2000;68(3):1026–33.
٥٧٥ 51. El-Kady IM. T-cell immunity in human chronic toxoplasmosis. J Egypt Soc Parasitol.
٥٧٦ 2011;41(1):17–28.
٥٧٧ 52. Suzuki Y, Orellana MA, Schreiber RD, Remington JS. In- terferon-gamma: the major
٥٧٨ mediator of resistance against *Toxoplasma gondii*. Science (80-). 1988;240(4851):516–8.

٥٧٩
٥٨٠
٥٨١
٥٨٢
٥٨٣
٥٨٤
٥٨٥
٥٨٦
٥٨٧
٥٨٨
٥٨٩
٥٩٠
٥٩١
٥٩٢

preprint